

Reconstitution and Characterization of Aminopyrrolnitrin Oxygenase, a Rieske *N*-Oxygenase That Catalyzes Unusual Arylamine Oxidation*[‡]

Received for publication, May 16, 2005, and in revised form, August 10, 2005. Published, JBC Papers in Press, September 2, 2006, DOI 10.1074/jbc.M505334200

Jungkul Lee¹, Michael Simurdiak, and Huimin Zhao²

From the Departments of Chemical and Biomolecular Engineering and Chemistry, Center for Biophysics and Computational Biology, Institute for Genomic Biology, University of Illinois, Urbana, Illinois 61801

Rieske oxygenases catalyze a wide variety of important oxidation reactions. Here we report the characterization of a novel Rieske *N*-oxygenase, aminopyrrolnitrin oxygenase (PrnD) that catalyzes the unusual oxidation of an arylamine to an aryl nitro group. PrnD from *Pseudomonas fluorescens* Pf5 was functionally expressed in *Escherichia coli*, and the activity of the purified PrnD was reconstituted, which required *in vitro* assembly of the Rieske iron-sulfur cluster into the protein and the presence of NADPH, FMN, and an *E. coli* flavin reductase SsuE. Biochemical and bioinformatics studies indicated that the reconstituted PrnD contains a Rieske iron-sulfur cluster and a mononuclear iron center that are formed by residues Cys⁶⁹, Cys⁸⁸, His⁷¹, His⁹¹, Asp³²³, His¹⁸⁶, and His¹⁹¹, respectively. The enzyme showed a limited range of substrate specificity and catalyzed the conversion of aminopyrrolnitrin into pyrrolnitrin with $K_m = 191 \mu\text{M}$ and $k_{\text{cat}} = 6.8 \text{ min}^{-1}$. Isotope labeling experiments with ¹⁸O₂ and H₂¹⁸O suggested that the oxygen atoms in the pyrrolnitrin product are derived exclusively from molecular oxygen. In addition, it was found that the oxygenation of the arylamine substrates catalyzed by PrnD occurs at the enzyme active site and does not involve free radical chain reactions. By analogy to known examples of arylamine oxidation, a catalytic mechanism for the bioconversion of amino pyrrolnitrin into pyrrolnitrin was proposed. Our results should facilitate further mechanistic and crystallographic studies of this arylamine oxygenase and may provide a new enzymatic route for the synthesis of aromatic nitro compounds from their corresponding aromatic amines.

The antibiotic pyrrolnitrin (3-chloro-4-(2'-nitro-3'-chlorophenyl)pyrrole) is produced by many *Pseudomonads* such as *Pseudomonas pyrocinia*, *Pseudomonas aureofaciens*, *Pseudomonas fluorescens*, and *Pseudomonas cepacia* and has broad spectrum antifungal activity (1–5). Biological activity of pyrrolnitrin at low concentrations was demonstrated to be due to the uncoupling of oxidative phosphorylation in *Neurospora crassa* and at higher concentrations due to inhibition of electron transport both in the flavin region and through cytochrome *c* oxidase (6). Recently, it was reported that pyrrolnitrin leads to glycerol accumulation and stimulation of triacylglycerol synthesis, resulting in

leaky cell membranes and concomitant breakdown of biosynthetic activity followed by cessation of cell growth (7).

The cloning and characterization of a 5.8-kb DNA region that encodes the pyrrolnitrin biosynthetic pathway was reported (8). This DNA region confers the ability to produce pyrrolnitrin when expressed heterologously in *Escherichia coli* and contains four genes, *prnABCD*, each of which is required for pyrrolnitrin production (9). A hypothetical biochemical pathway for the synthesis of pyrrolnitrin has been proposed by van Pée *et al.* (10). In this pathway shown in Fig. 1, the first step is the chlorination of tryptophan by PrnA at the 7 position to form 7-chlorotryptophan, followed by rearrangement of the indole ring to a phenylpyrrole ring and decarboxylation by PrnB to form monodechloroaminopyrrolnitrin. This intermediate is chlorinated a second time by PrnC to form aminopyrrolnitrin, which, in the last step of the pathway, undergoes oxidation of the amino group in aminopyrrolnitrin to a nitro group by PrnD to form pyrrolnitrin.

The biosynthesis of pyrrolnitrin is one of the best examples of enzyme-catalyzed arylamine oxidation. Although arylamine oxygenases seem to be widely distributed within the microbial world and used in a variety of metabolic reactions (11–16), PrnD represents one of only two known examples of arylamine oxygenases or *N*-oxygenases involved in aryl nitro group formation, the other being AurF involved in aureothin biosynthesis (16, 17). The nitro group plays an important role in their activity. Pyrrolnitrin analogues containing an amino group instead of a nitro group have no inhibiting effect on the growth of *Neurospora crassa* (18). Sequence analysis suggested that PrnD is a Rieske oxygenase consisting of a consensus Rieske [2Fe-2S] cluster-binding motif and a mononuclear non-heme Fe(II)-binding motif DXXHXXXXH (8). Rieske oxygenases are widespread in nature and catalyze a diverse set of oxidation reactions including *cis*-dihydroxylation, monohydroxylation, desaturation, sulfoxidation, and *O*- and *N*-dealkylation (19, 20). However, because of the difficulties in protein expression and purification, arylamine oxygenases involved in aryl nitro group formation including PrnD have never been characterized and assigned a defined function.

Here we report for the first time the functional expression, purification, reconstitution, and characterization of a novel Rieske *N*-oxygenase, PrnD, that catalyzes unusual arylamine oxidation. To explore the mechanism of its reaction further, we describe *in vitro* oxygenation of the precursor arylamine to an aryl nitro product by purified and reconstituted PrnD, which has one Rieske-type [2Fe-2S] center and one mononuclear iron site/monomer. We also suggest the origin of oxygen in the nitro group and the putative mechanism for arylamine oxidation by PrnD.

EXPERIMENTAL PROCEDURES

Materials—The pMal-c2x expression vector, *malE* primer, factor Xa, amylose resin, Taq DNA polymerase, T4 DNA ligase, DNase I, and

* This work was supported by Office of Naval Research Grant N00014-02-1-0725. The costs of publication of this article were defrayed in part by the payment of page charges. This article must therefore be hereby marked "advertisement" in accordance with 18 U.S.C. Section 1734 solely to indicate this fact.

[‡] The on-line version of this article (available at <http://www.jbc.org>) contains a supplemental table and supplemental figures.

¹ Supported in part by the Korea Research Foundation Grant funded by Korea Government (Basic Research Promotion Fund Grant MOI-2004-000-10159-0).

² To whom correspondence should be addressed: Dept. of Chemical and Biomolecular Engineering and Chemistry, Center for Biophysics and Computational Biology, Institute for Genomic Biology, University of Illinois, 600 S. Mathews Ave., Urbana, IL 61801. Tel.: 217-333-2631; Fax: 217-333-5052; E-mail: zhao5@uiuc.edu.

Characterization of Aminopyrrolinrin Oxygenase

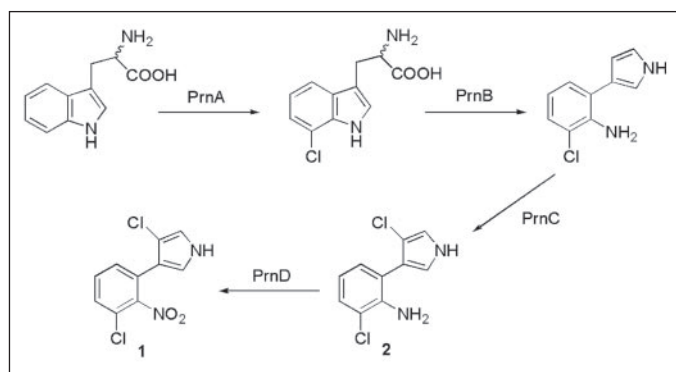


FIGURE 1. Proposed biosynthetic pathway for pyrrolinrin (10).

restriction endonucleases were purchased from New England Biolabs (Beverly, MA). Plasmid pQE-80L was obtained from Qiagen. Plasmid pTKXb119 was a kind gift of Dr. K. H. Park at Seoul National University (Seoul, Korea). $^{18}\text{O}_2$ (97% O^{18} -enriched), H_2^{18}O (97% O^{18} -enriched), superoxide dismutase (2500 units/mg), xanthine oxidase (7 units/mg), catalase (10,000 units/mg), BCA protein assay kit, mannitol, and pyrrolinrin were from Sigma. Materials for PCR product purification, gel extraction, and plasmid preparation were obtained from Qiagen. Oligonucleotide primers were obtained from Integrated DNA Technologies (Coralville, IA). The physiological substrate, aminopyrrolinrin (3 mg), was a kind gift of Dr. J. W. Frost at Michigan State University (East Lansing, MI). Substrate analogues (4-amino-L-phenylalanine, 2-amino-3-chlorobenzoic acid, 3-amino-4-chlorobenzoic acid, 3-amino-4-chlorophenol, 4-aminobenzamide dihydrochloride, 4-aminobenzyl amine, 3-aminobenzoic acid, 4-aminobenzoic acid, 4-aminobenzamide, aniline, 4-aminoacetophenone, 4-aminoacetanilide, 3-amino-acetanilide, 1,2-phenylenediamine, 1,3-phenylenediamine, 1,4-phenylenediamine, 1,3,5-triamino-benzene), and the corresponding nitro compounds including 4-nitrobenzyl amine were from Aldrich.

Bacterial Strains and Growth Conditions—*E. coli* BL21 (DE3) and DH5 α were obtained from Novagen (Madison, WI) and the Media Preparation Facility of the University of Illinois Biochemistry Department (Urbana, IL), respectively. *P. fluorescens* Pf-5 (number BAA-447) was purchased from the American Type Culture Collection (Manassas, VA). *E. coli* strains DH5 α and BL21(DE3) were grown aerobically at 37 °C or 30 °C in Luria-Bertani medium with constant shaking (220 rpm). When necessary, kanamycin was added at 50 $\mu\text{g}/\text{ml}$ and ampicillin at 100 $\mu\text{g}/\text{ml}$. The solid media were prepared by the addition of 1.5% (w/v) agar.

Construction of the pMAL-c2x-prnD Expression Plasmid—The *prnD* gene was amplified by PCR from *P. fluorescens* Pf-5 genomic DNA using two oligonucleotide primers 5'-GGGGATCCATGAACGACATTCAATTGGATCAAG-3' (BamHI restriction site is underlined) and 5'-GGAAGCTTTCACCGCTCACTTGCGACGCG-3' (HindIII restriction site is underlined). The PCR amplification was carried out using *Pfu* Turbo DNA polymerase (Stratagene, La Jolla, CA) to minimize potential point mutations introduced by PCRs under standard conditions (21). The PCR program was 2 min at 96 °C followed by 30 cycles of 1 min at 94 °C, 1 min at 48 °C, 2 min at 72 °C, and a final elongation of 7 min at 72 °C. The PCR products were cleaved by BamHI and HindIII and purified using QIAEX II gel purification kit (Qiagen). The purified product was cloned into the BamHI- and HindIII-digested expression vector pMal-c2x. The resulting pMal-c2x-prnD is under the control of the *tac* promoter and expresses PrnD as a fusion protein to the C terminus of

the maltose-binding protein (MBP).³ The cloned *PrnD* gene was confirmed to be free of point mutations by DNA sequencing at the Biotechnology Center of the University of Illinois using the Big DyeTM Terminator sequencing method and an ABI PRISM[®] 3700 sequencer (Applied Biosystems, Foster City, CA).

Expression and Purification of the Fusion Protein—Overnight cultures of BL21 (DE3) cells transformed with the pMal-c2x-prnD vectors were diluted 1:200 into LB medium supplemented with ampicillin (100 $\mu\text{g}/\text{ml}$) and grown at 30 °C until absorbance at 600 nm (A_{600}) reached ~ 0.6 . Then protein expression was induced by the addition of isopropyl- β -D-1-thiogalactopyranoside to 0.1 mM final concentration, and the incubation was continued for 3 h. The cells were harvested by centrifugation at 4 °C for 20 min at 6,000 $\times g$, rinsed with phosphate-buffered saline, and frozen and stored at -20 °C. The yield was ~ 3 g of bacterial wet weight/liter of culture. A bacterial lysate was prepared by thawing and resuspending cells from a 1-liter culture in 40 ml of buffer containing 20 mM Tris-HCl, pH 7.5, 1 mM dithiothreitol, 100 mM NaCl, 1 mM phenylmethanesulfonyl fluoride, and 0.1 mM EDTA (starting buffer); this suspension was treated with 10 mg of lysozyme for 30 min. The suspension was sonicated on ice with a Branson sonicator for 1 min five times at 1-min intervals. After centrifugation for 20 min at 10,000 $\times g$, the supernatant was adjusted to 0.5 M NaCl and loaded onto an amylose resin column (3 mg of fusion protein/ml of amylose). The column was washed with 10 volumes of 0.5 M NaCl in starting buffer and with 20 volumes 20 mM Tris-HCl, pH 7.8, 100 mM NaCl, 1 mM dithiothreitol, before eluting with 10 mM maltose in the latter buffer. For cleavage with factor Xa, the dialyzed MBP-prnD fusion protein was incubated with factor Xa (1 $\mu\text{g}/200$ μg of fusion protein) for 16 h at 4 °C. Maltose was removed by hydroxyapatite resin, and MBP was removed after cleavage by a second adsorption to the amylose resin. Fractions from the amylose column were then concentrated with Centricon-10 ultrafiltration units (Amicon), adjusted to 100 mM NaCl, 20 mM Tris, 1 mM dithiothreitol, pH 7.8.

Construction of the pTKXb-prnD Plasmid and Its Expression and Purification—The PCR product obtained by using the oligonucleotide primers 5'-GGCATATGAACGACATTCAATTGGATCAAG-3' (NdeI restriction site is underlined) and 5'-GGCTCGAGTCACCGCTCACTTGCGACGCG-3' (XhoI restriction site is underlined) was cleaved by NdeI and XhoI and purified using QIAEX II gel purification kit (Qiagen). The purified product was cloned into the NdeI- and XhoI-digested expression vector p6xHTKXb119 (22) to give pTKXb-prnD, which was transformed into *E. coli* BL21 (DE3). In this expression plasmid, the *prnD* gene was placed under the transcriptional control of the promoter P_{BLMA} from *Bacillus licheniformis*, which is constitutively induced in *E. coli* (23).

For the purification of His₆-tagged TKXb-PrnD protein, 3 g of *E. coli* cells cultured for 24 h were resuspended in 10 ml of binding buffer (5 mM imidazole, 0.5 M NaCl, 20 mM Tris-HCl, pH 7.9) supplemented with 25 $\mu\text{g}/\text{ml}$ DNase I and disrupted by the same method as described above. After clarification by centrifugation for 30 min at 20,000 $\times g$ and 4 °C, the volume of the crude extract was adjusted to 10 ml with binding buffer. The crude extract was then loaded at a flow rate of 25 ml/h onto a 2.5-ml HisBind Resin column (Novagen, Madison, WI), which had been activated with NiSO₄ and equilibrated with binding buffer as described by the manufacturer. The sample was washed with 10 column volumes of binding buffer, followed by washing with 6 column volumes of wash buffer (60 mM imidazole, 0.5 M NaCl, 20 mM Tris-HCl, pH 7.9).

³ The abbreviations used are: MBP, maltose-binding protein; HPLC, high pressure liquid chromatography.

An additional wash step with a buffer containing 100 mM imidazole was performed for 6 column volumes prior to PrnD elution with 200 mM imidazole, 0.5 M NaCl, 20 mM Tris-HCl, 20% glycerol, pH 7.9. The protein solution was stored at -20°C until further use.

Site-directed Mutagenesis of pTKXb-PrnD—Site-directed mutagenesis was carried out by using a QuikChange site-directed mutagenesis kit from Stratagene. The pTKXb-prnD plasmid was used as the DNA template. Two conserved Cys residues (Cys⁶⁹ and Cys⁸⁸) in the iron-sulfur cluster and two Asp residues (Asp³²³ and Asp³³³) were mutated to Ala individually. The plasmids containing the correct mutant genes were then used to transform *E. coli* BL21(DE3), and colonies selected by kanamycin resistance were used for protein expression. The pTKXb-PrnD mutants were expressed according to the same procedure for the wild type enzyme as described above.

In Vitro Reconstitution of the Iron-Sulfur Clusters into the PrnD Proteins—The reconstitution procedures (24–27) were carried out in an anaerobic chamber (Jacomex, Dagneux, France). All of the solutions were incubated anaerobically for 2 h before the beginning of each experiment. The purified PrnD was diluted to 10–20 μM with N_2 -sparged 20 mM Tris-HCl buffer (pH 7.8) containing 10 mM dithiothreitol, 200 mM NaCl, 0.5 mM EDTA, 1 mM phenylmethanesulfonyl fluoride, and 10% (v/v) glycerol. β -Mercaptoethanol was added to the protein solution at 1.0% (v/v), and the solution was gently mixed and left for 90 min. $\text{Fe}(\text{NH}_4)_2(\text{SO}_4)_2$ and Na_2S were added to the solution at a final concentration of ~ 1.0 mM. The reconstitution proceeded for 2–3 h. The solution was diluted 8-fold by the addition of N_2 -sparged 20 mM Tris-HCl buffer (pH 7.8), further diluted 2-fold by the addition of 20 mM Tris-HCl buffer (pH 7.8) equilibrated in air, and then dialyzed against the same buffer. Excess Fe^{2+} and S^{2-} were removed by a desalting column (Bio-Rad; 10-DG). The reconstituted PrnD protein was concentrated on Centricon-30 ultrafiltration units (Amicon, Beverly, MA) to a final volume of 0.2 ml and stored at 4°C or for longer periods at -80°C . The iron-sulfur cluster incorporation was analyzed by EPR spectroscopy.

Construction of pQE-ssuE Expression Plasmid—For the production of SsuE reductase, the *ssuE* gene was placed under the control of the T5 RNA polymerase promoter using vector pQE-80L. The *ssuE* gene was amplified by PCR from *E. coli* XL1 Blue genomic DNA using the two oligonucleotide primers 5'-GGCATATGCGTGTCATCACCCCTGGC-3' (NdeI restriction site is underlined) and 5'-GGAAGCTTTTACGCATGGGCATTACCTC-3' (HindIII restriction site is underlined). The 672-base pair PCR product was digested with NdeI and HindIII, and the resulting fragment was ligated in pGEMT-easy to form plasmid pGEMTssuE. For the production of SsuE as an N-terminal His₆-tagged fusion protein, the NdeI-HindIII SsuE-encoding fragment from plasmid pGEMTssuE was ligated into NdeI-HindIII-digested pQE-80L to form plasmid pQE-ssuE.

Production and Purification of SsuE Protein—*E. coli* BL21(DE3) containing the appropriate overexpression plasmid pQE-ssuE was grown at 30°C and 220 rpm in a 2-liter Erlenmeyer flask containing 400 ml of growth medium. To minimize the formation of insoluble protein aggregates, which were observed when protein production was carried out at 30°C , cultures grown to an A_{600} of 0.5 were cooled to 16°C , induced by the addition of isopropyl- β -D-1-thiogalactopyranoside to a final concentration of 100 mM and incubated for a further 5 h at 16°C with constant shaking (220 rpm). The cells were collected by centrifugation for 20 min at $6000 \times g$ and 4°C , washed in an excess of 20 mM Tris-HCl buffer, pH 7.9, and stored at -20°C as frozen pellets until further use. About 4 g of fresh weight of cells was collected from a 1000-ml culture. SsuE protein was purified as described under "Construction of the pTKXb-prnD Plasmid and Its Expression and Purification."

Reconstitution of PrnD Activity—PrnD activity was routinely assayed with HPLC. The assay mixture (final volume, 0.5 ml) contained 100 μM NADPH, 3 μM FMN, 500 μM substrate, SsuE and PrnD to a SsuE/PrnD molar ratio of 4.0 in 20 mM Tris-HCl, pH 7.8, and was stirred at 30°C . The reactions were started by the addition of PrnD to the reaction mixture and analyzed by HPLC. One unit of activity was defined as the amount of enzyme forming 1 μmol of product/min at 30°C under standard assay conditions, calculated from the rate of substrate depletion.

Activity Assay of PrnD with Superoxide Dismutase, Xanthine Oxidase, and Hydroxyl Radical Scavengers—Superoxide dismutase was added to some of the incubation mixtures. After a 5-min preincubation at 30°C with shaking, the reaction was started by the addition of aminopyrrolnitrin (1 mM). The reaction was run for 30 min and was terminated by pouring the incubation mixture into 10 ml of ice-cold dichloromethane that had previously been bubbled with N_2 for 20 min and analyzed by HPLC. Incubation mixtures for the xanthine/xanthine oxidase system in 20 mM Tris-HCl buffer (pH 7.8) contained 75 μM of xanthine, 5 units of xanthine oxidase, and 1 mM of aminopyrrolnitrin in a final volume of 300 μl . Catalase, mannitol, or Me_2SO were also included in some incubation mixtures. After a 5-min preincubation at 30°C , the reaction was started by the addition of substrate, allowed to proceed for 30 min, and stopped and analyzed as described above. The production of pyrrolnitrin was linear under these conditions for at least 30 min.

Protein Electrophoresis and Immunoblotting—SDS-PAGE and immunoblot analyses were performed largely as described by Sambrook *et al.* (21). SDS-PAGE was performed on a Mini-PROTEAN II system (Bio-Rad) with 12% polyacrylamide gels (30% acrylamide, 0.8% bis-acrylamide stock) under denaturing conditions. Protein concentrations were measured using the method of BCA (Sigma) according to the manufacturer's instructions with bovine serum albumin as a standard. Samples for SDS-PAGE were incubated, typically 5 min at 90 – 100°C , with an equal volume of denaturing sample buffer. Broad range molecular weight standards were purchased from Bio-Rad. Proteins from gels were transferred electrophoretically onto a polyvinylidene difluoride membrane (Amersham Biosciences). Nonfat dry milk was used as the blocking agent. The His-Tag[®] monoclonal primary antibody (Novagen, Madison, WI) and the secondary mouse IgG alkaline phosphatase conjugate (Sigma) were used at 1:10,000 and 1:20,000 dilutions, respectively. Cross-reacting protein bands were visualized with 5-bromo-4-chloro-3-indolyl phosphate (0.17 mg/ml) and nitro blue tetrazolium (0.33 mg/ml) purchased from Sigma.

Enzyme Kinetics and pH Profiles of the Kinetic Parameters—Kinetic parameters determined in atmospheric oxygen were obtained by fitting the data to the Michaelis-Menten equation. To determine the kinetic constants for oxygen, the oxygen was removed from the enzyme reaction mixture by alternately filling and evacuating the vessel containing the reaction mixture with pure nitrogen. Different oxygen concentrations were bubbled through the substrate solutions for at least 10 min to obtain final oxygen concentrations of 0.03, 0.06, 0.12, and 0.6 mM. The concentrations of the arylamines varied from 20 μM to 5 mM.

For assays at different pH values, the reactions were performed in the following buffers (50 mM) and pH values: sodium citrate (pH 5.0–5.5), potassium phosphate (pH 6.0–6.8), Tris/HCl (pH 7.0–9.0), and glycine/NaOH (pH 9.5–10.0). To construct the pH profiles, the kinetic parameters k_{cat} and k_{cat}/K_m for aminopyrrolnitrin were determined between pH 5.0 and 9.5, and the pH dependence of $Y(k_{\text{cat}}/K_m)$ was fitted to a bell-shaped curve described by Equation 1, which describes a bell-

Characterization of Aminopyrrolnitrin Oxygenase

shaped curve with a slope of +1 at low pH and a slope of -1 at high pH,

$$\log Y = \log[Y_H/(1 + H/K_1 + K_2/H)] \quad (\text{Eq. 1})$$

where H is the proton concentration, K_1 and K_2 are the dissociation constants for the groups that ionize at low and high pH, respectively, and Y_H is the pH-independent plateau value of Y at intermediate pH. The pH profile for k_{cat} was constructed in a point-to-point manner.

Analytical Methods—Optical spectra were recorded on a Varian Cary 100 Bio UV-visible spectrophotometer. ^1H NMR spectra (500 MHz) were measured with a DXR 500 AVANCE spectrometer from Bruker Instruments (Karlsruhe, Germany). EPR samples were prepared in an anaerobic chamber. The protein solution was transferred to an EPR tube, and after 5–10 min of incubation at room temperature, the samples were quickly frozen and stored in liquid nitrogen until EPR analyses. EPR measurements were performed on a Varian E-122 X-band spectrometer equipped with an Air Products Helitran cryostat. Other parameters for the measurement include 2-milliwatt microwave power, 2-G modulation amplitude, and 9.08-GHz microwave frequency. The spectra were acquired at 15 K. Spin concentrations were determined by double integrating base line-corrected spectra. For calibration, a sample containing 1 mM CuSO_4 in a 20% glycerol solution was run at the same power and temperature used for the protein samples. Mononuclear iron content was determined as described previously (28). Potentiometric redox titrations monitored by EPR were performed using sodium dithionite anaerobically in 20 mM buffer at pH 7. PrnD protein concentration was 56 μM . The following redox mediators were used: methyl viologen, benzyl viologen, neutral red, anthraquinone-2-sulfonate, anthraquinone-1,5-disulfonate, 2-hydroxy-1,4-naphthoquinone, 2,5-dihydroxy-*p*-benzoquinone, phenazine methosulfate, menadione, and duroquinone, each at a concentration 50 μM .

Acid-labile sulfide was determined as described elsewhere (29). Enzyme reaction products were analyzed and purified by an Agilent 1100 Series HPLC System. The sample was eluted on a ZORBAX SB-C8 Column (4.6 \times 150 mm, Agilent). HPLC parameters were as follows: 25 $^\circ\text{C}$; solvent A, 1% acetic acid in water; solvent B, methanol; gradient, 5% B for 2 min; then to 100% B in 18 min and finally maintain at 100% B for 2 min; flow rate 1.0 ml/min; detection was by UV spectroscopy at 254 nm.

Reactions in the Presence of $^{18}\text{O}_2$ —Two vials, one containing aminopyrrolnitrin and one containing the holo-PrnD reaction mixture, were degassed by application of a vacuum and flushed with argon for three times. The anaerobic holo-PrnD solution was transferred to the substrate vial containing aminopyrrolnitrin. The argon was removed by application of a vacuum, and finally $^{18}\text{O}_2$ was allowed to enter into the vial. After incubation for 1 h at 30 $^\circ\text{C}$, the reaction was analyzed by HPLC coupled to an electrospray ionization mass spectrometer (TSQ Quantum; ThermoFinnigan, San Jose, CA) in positive ion mode. A linear gradient of MeOH (0–75%) in 0.1% aqueous acetic acid was used.

RESULTS

Cloning and Heterologous Expression of PrnD—One of the most critical limitations for biochemical and mechanistic studies of PrnD to date has been the lack of an efficient method to obtain large amounts of purified enzymes. Indeed, soluble expression of PrnD has never been reported. In the present study, the gene encoding PrnD was amplified from *P. fluorescens* Pf-5 genomic DNA using PCR and cloned into the expression vectors pTKXb119 and pMal-c2x to give the plasmids pTKXb-prnD and pMal-c2x-prnD, respectively. Among them, the constitutive expression of the plasmid pTKXb-prnD with the N-terminal His₆ tag in *E. coli* BL21(DE3) led to the soluble production of a protein of

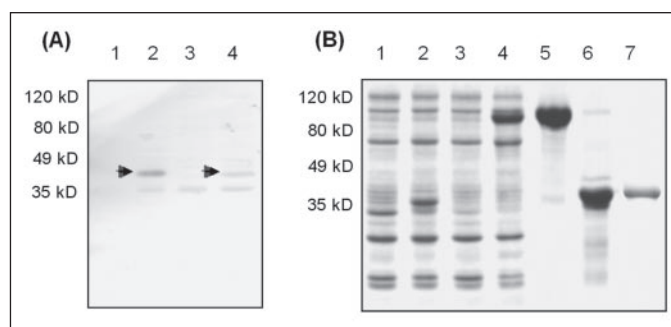


FIGURE 2. Immunoblot (A) and SDS-PAGE analysis (B) of isolated *E. coli* cell harboring pTKX-prnD and pMal-c2x-prnD, respectively. A, immunoblot. Lane 1, control total fraction; lane 2, total fraction; lane 3, control soluble fraction; lane 4, soluble fraction. For immunodetection, polyclonal antibody against His₆ tag protein was used. B, SDS-PAGE. Lane 1, pMal-c2x control total fraction; lane 2, pMal-c2x control soluble fraction; lane 3, pMal-c2x-prnD total fraction; lane 4, pMal-c2x-prnD soluble fraction; lane 5, maltose eluate of MBP-PrnD; lane 6, products of factor Xa cleavage of MBP-PrnD; lane 7, PrnD purified by the second amylose resin.

expected size \sim 41 kDa that cross-reacted with a His₆ tag-specific antibody but only at a low level requiring immunological detection (Fig. 2A, lane 4). The overall protein yield of pTKXb-PrnD (below 0.1 mg of purified PrnD obtained per liter of culture) was too low to be used for characterization of PrnD. Instead, a large amount of purified PrnD was obtained from the cleavage of MBP-PrnD fusion protein followed by affinity chromatography as described under “Experimental Procedures.” Induction of the plasmid pMal-c2x-prnD with 0.1 mM isopropyl- β -D-1-thiogalactopyranoside at 20 $^\circ\text{C}$ led to the overproduction of soluble MBP-PrnD fusion protein of expected size \sim 85 kDa (Fig. 2B, lane 4). Induction of empty plasmid pMAL-c2x produced \sim 40 kDa proteins of the size expected for MBP alone (Fig. 2B, lane 2). After purification, MBP was cleaved from PrnD by Factor Xa treatment and removed. This procedure resulted in apparently homogenous PrnD protein as judged by SDS-PAGE (Fig. 2B, lane 7). The molecular mass observed in SDS-PAGE corresponded to the calculated mass of the protein (41 kDa). A protein yield of \sim 7 mg of pure PrnD/liter of culture was obtained. By using gel filtration chromatography, the molecular mass of native PrnD was determined as 86 kDa, showing that the protein is homodimeric in solution.

Reconstitution of PrnD with Reductase and Rieske [2Fe-2S] Cluster—Rieske oxygenases are typically comprised of two protein components: a terminal oxygenase containing a Rieske iron-sulfur cluster and a non-heme iron active site and a reductase containing flavin (30). Thus, a reductase was deemed necessary for the function of PrnD. Because the flavin reductase was known to be non-specific (31), the unknown reductase for PrnD from the *Pseudomonas* strain was substituted by flavin reductase SsuE from *E. coli*. Induction of the plasmid pQE-ssuE in *E. coli* BL21(DE3) led to soluble SsuE protein production of expected size \sim 25 kDa, which was purified by nickel-nitrilotriacetic acid affinity chromatography (Fig. 3). However, PrnD protein cleaved from MBP-PrnD did not show any activity in combination with SsuE reductase, NADPH, and FMN. In addition, we were unable to detect the characteristic $g = \sim$ 1.9 EPR signal corresponding to Rieske proteins directly from PrnD cleaved from MBP-PrnD overproduced in *E. coli*. We therefore pursued *in vitro* reconstitution of the Rieske [2Fe-2S] cluster with reduced iron and sulfide as described under “Experimental Procedures.” This approach allowed assembly of the characteristic Rieske [2Fe-2S] cluster into the overproduced PrnD protein as demonstrated by the following spectroscopic analyses. In addition, the color of the reconstituted PrnD proteins was brown, indicating the presence of an iron-sulfur cluster.

Spectral Characterization of a Rieske [2Fe-2S] Cluster in Reconstituted PrnD—Fig. 4 shows the optical spectra of reconstituted PrnD. Although the spectrum of the reconstituted and air-oxidized PrnD

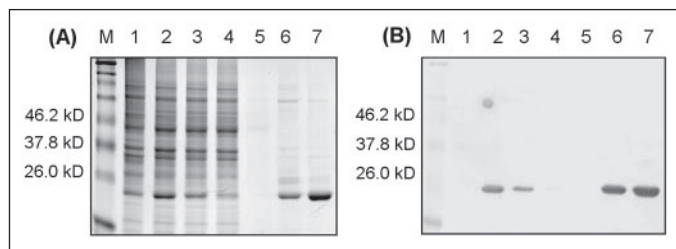


FIGURE 3. Expression and purification of SsuE reductase from *E. coli*. *A*, SDS-PAGE. Protein samples (20 μ g) were analyzed at different stages on 12% SDS-PAGE gels under reducing and denaturing conditions and stained with Coomassie Brilliant Blue. Lane *M*, molecular mass markers (with molecular masses indicated on the left in kDa); lane 1, cell extract of uninduced *E. coli* BL21(DE3) (pQE-ssuE); lane 2, total extract of cells producing SsuE from pQE-ssuE; lane 3, soluble extract of induced *E. coli* BL21(DE3)(pQE-ssuE) cells producing His₆-tagged SsuE; lane 4, flow through; lane 5, wash with binding buffer; lane 6, eluate with 200 mM imidazole; lane 7, eluate with 250 mM imidazole. *B*, immunoblot. See description for *A*.

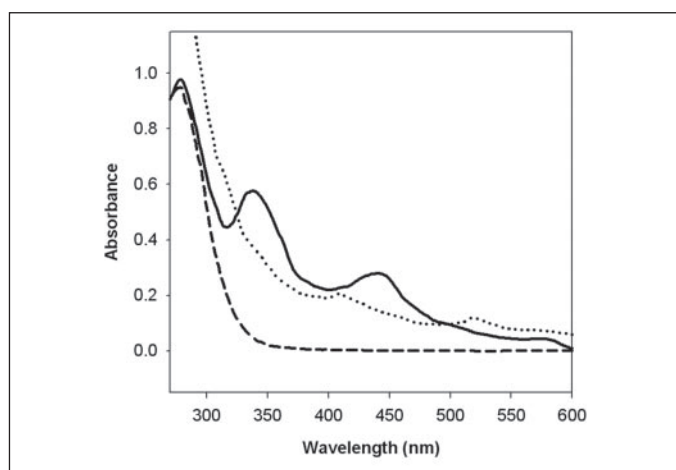


FIGURE 4. UV-visible spectra of PrnD as purified and PrnD after reconstitution of Rieske [2Fe-2S] cluster. The solid line is the spectrum of reconstituted PrnD, the dashed line is the spectrum of PrnD of the reconstituted and oxidized PrnD, and the dotted line is the spectrum of the reconstituted and reduced PrnD.

shows absorption maxima at 278, 339, and 440 nm and a distinct shoulder at 570 nm, the spectrum of the reconstituted and dithionite reduced PrnD shows absorption maxima at 405 and 521 nm, which are most similar to those of the [2Fe-2S] proteins with the Rieske-type [2Fe-2S] cluster (30, 32) and distinctively different from those of the bacterium-type ferredoxins or rubredoxins (33). The extinction coefficient of oxidized PrnD at 440 nm, ϵ ([2Fe-2S]) of $6.5 \text{ mM}^{-1} \text{ cm}^{-1}$ (mean from three different preparations), is similar to that at 458 nm for *Thermus thermophilus* Rieske protein ($6.0 \text{ mM}^{-1} \text{ cm}^{-1}$) (32). The optical spectrum was not affected by dialysis against an EDTA-containing buffer. PrnD is also readily reducible by sodium ascorbate in 5 min, suggesting that the redox center has a reduction potential well above 0 V, as is the case for the respiratory Rieske-type [2Fe-2S] proteins (32) and much higher than those of the [2Fe-2S] centers of the plant-type ferredoxins (30). Coordination of Rieske clusters by His imidazole nitrogen as well as Cys sulfur ligands is thought to account in part for the high potentials (-140 to $+320$ mV) of Rieske [2Fe-2S] centers relative to -270 to -460 mV in plant, vertebrate, and bacterial [2Fe-2S] ferredoxins (34, 35).

Fig. 5A shows the X-band EPR spectrum of reconstituted PrnD at 15 K. Although the air-oxidized form of PrnD as it is isolated is diamagnetic (EPR silent) and does not elicit any adventitious Fe^{3+} signal at a g of 4.3, indicating the absence of any rubredoxin-like iron center, the protein reconstituted and fully reduced by excess dithionite elicits a rhombic $S = 1/2$ resonance with principal $g_{x,y,z}$ values of 1.78, 1.89, and

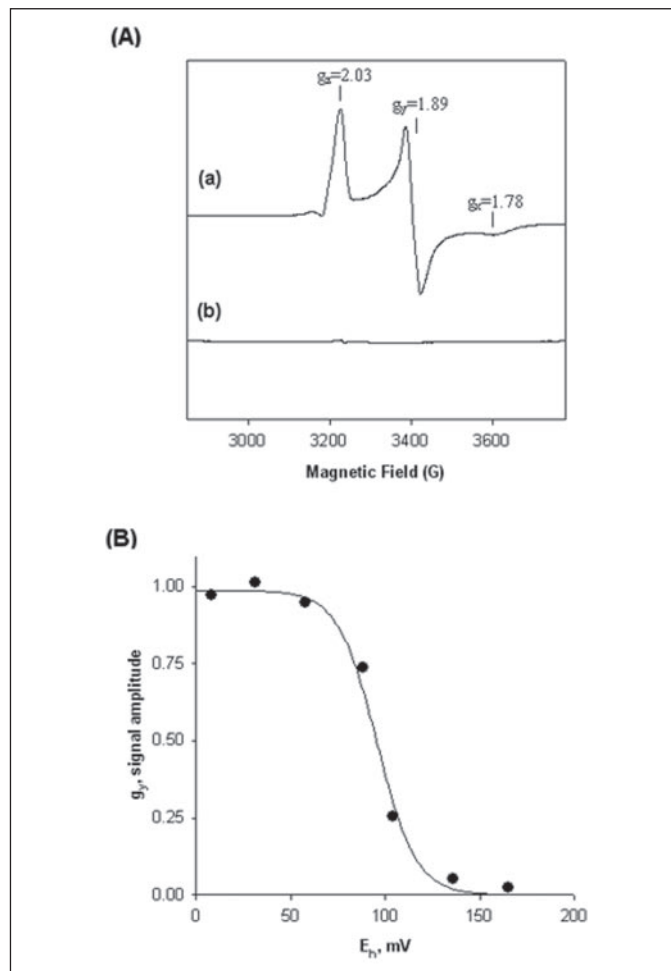


FIGURE 5. A, comparison of EPR spectra between PrnD after reconstitution of iron-sulfur cluster (spectrum *a*) and PrnD as purified (spectrum *b*). The concentration of protein was ~ 0.5 mM protein. The conditions of recording were: microwave power, 6.3 milliwatt; microwave frequency, 9.44 GHz; modulation amplitude, 10 G at 100 kHz; scan rate, 250 or 125 G/min; and $T = 15$ K. The $g_x = 1.78$, $g_y = 1.89$, and $g_z = 2.03$ resonances are characteristic of the Rieske [2Fe-2S] cluster. **B**, potentiometric redox titration of PrnD measured by EPR at pH 7.0. Titrations were performed anaerobically as described under "Experimental Procedures."

2.03 (Fig. 5A), which could be readily detected at temperatures at least up to 70 K, as in the cases of some [2Fe-2S] clusters (32, 36). In addition, its unusually low g_{av} value (1.90) is comparable with that of the Rieske-type [2Fe-2S] clusters ($g_{av} = \sim 1.91$) (34, 37). The EPR spectra of reduced PrnD were very similar to those of the Rieske-type [2Fe-2S] protein from *T. thermophilus* (30), phthalate oxygenase, and iron-sulfur-containing oxygenases isolated from Pseudomonads (38–42), indicating that PrnD contains a Rieske-type [2Fe-2S] center. The redox potential was determined through titration of PrnD with different redox mediators. The titration was followed through EPR, and a redox midpoint potential of 95 mV was found (Fig. 5B).

The metal analysis of reconstituted PrnD by inductively coupled plasma atomic emission spectrometry showed the presence of tightly bound iron that was not removable by dialysis for 2 days against 20 mM Tris-HCl buffer (pH 7.8) containing 1 mM EDTA. The iron contents of PrnD as isolated and PrnD after dialysis against EDTA were determined to be 2.9 and 2.1 mol of iron/mol of monomer, respectively. Reconstituted PrnD also contained 1.9 mol of acid-labile sulfide/mol of monomer (means from three different preparations), presumably indicating an sulfur/iron ratio of 1 for the protein after dialysis against EDTA.

Characterization of Aminopyrrolnitrin Oxygenase

Thus, these data indicate that PrnD contains one [2Fe-2S] cluster and one mononuclear non-heme iron center/41-kDa monomer.

Requirement of the Mononuclear Iron Site—The EPR signals in the reduced wild type PrnD were quantified by double integration and compared with a copper sulfate standard. To quantitate the spin concentrations associated with the EPR signals, a sample of the reconstituted and reduced PrnD with a protein and iron concentrations of 46 and 133 μM , respectively, was used. The spin concentration was 45 μM corresponding to the [2Fe-2S] ($S = \frac{1}{2}$) signal. Whereas total iron concentration was decreased to 96 μM after dialysis against EDTA, the spin concentration was not changed after dialysis. The spin concentration of the [2Fe-2S] center is approximately equal to that of the PrnD protein ($\pm 10\%$). These results reinforce the conclusion that the [2Fe-2S] is a *bona fide* component of the enzyme. The mononuclear iron occupancy (43 μM) determined by subtracting the Rieske iron content (90 μM , each $S = \frac{1}{2}$, spin = 2.0 iron) from the total iron (133 μM) was $\sim 90\%$ of the theoretical value.

Enzyme with about 3 atoms of iron/PrnD monomer had full PrnD activity when assayed in the absence of Fe^{2+} . The removal of the mononuclear iron by dialysis against EDTA from PrnD led to the significant loss of activity ($>90\%$), and the incubation with Fe^{2+} caused nearly maximal reactivation of PrnD, indicating the necessity of the mononuclear iron for enzyme activity. Other samples with intermediate Fe/PrnD ratios (between 2 and 3) were prepared by incubating EDTA-treated PrnD with various levels of Fe^{2+} . The specific activity of these samples was proportional to the iron content over the range from 2 to 3 total atoms of iron/PrnD monomer. Taken together, these data indicate the requirement of mononuclear iron site for PrnD activity.

Characterization of the Reconstituted PrnD and Its Reaction Product—The physiological substrate aminopyrrolnitrin was used to check whether the Rieske iron-sulfur cluster reconstituted PrnD was indeed able to catalyze an arylamine oxidation in combination with SsuE reductase *in vitro*. Although no activity was observed when aminopyrrolnitrin alone was used as a substrate, PrnD showed significant activity when SsuE, FMN, and NADPH were used for reconstitution, producing a compound that migrated on HPLC at the same retention time (15.94 min) as authentic pyrrolnitrin. To verify the identity of this compound produced by PrnD, it was purified by HPLC as mentioned under "Experimental Procedures," and this compound was unambiguously identified as pyrrolnitrin by ^1H NMR and high resolution electron ionization mass spectrometry. (^1H NMR (Acetone- d_6 , 500 MHz) δ (ppm) 6.91 (m, 1H), 7.02 (m, 1H), 7.65 (m, 4H); HR EI-MS, calculated for pyrrolnitrin (M^+) 255.9806, found 255.9808.) ^1H NMR spectrum of the isolated product was identical to spectra previously reported for pyrrolnitrin (43). Taken together, these results clearly indicate that the product of the prnD gene is an arylamine oxygenase, aminopyrrolnitrin oxygenase.

Enzyme Kinetics and pH Profiles of the Kinetic Parameters—An increase in PrnD activity with increasing SsuE concentration was observed with saturation after the SsuE/PrnD molar ratio reaches ~ 3.0 .

Thus, at a SsuE/PrnD molar ratio of 4.0, initial velocity studies were performed with aminopyrrolnitrin as a variable substrate in the presence of fixed concentration of PrnD ($\sim 1 \mu\text{M}$). Values of $K_m = 191 \mu\text{M}$ for aminopyrrolnitrin and a $k_{\text{cat}} = 6.8 \text{ min}^{-1}$ (specific activity = 0.08 unit/mg protein) were determined for PrnD. This heterologously expressed and reconstituted PrnD showed a comparable activity to the native PrnD enzyme in *P. fluorescens* Pf5 (specific activity = 0.10 unit/mg protein), indicating that mononuclear iron atoms are present in high occupancy.

To give further insight into the mechanism of PrnD, the variation of kinetic parameters with pH was studied. The pH profiles of the kinetic parameters using aminopyrrolnitrin as a substrate are shown in Fig. 6. The effect of pH on the ionization of free *P. fluorescens* PrnD was visualized by the plot of $\log k_{\text{cat}}/K_m$ ($\text{M}^{-1} \text{s}^{-1}$) versus pH. The pH profile of $\log k_{\text{cat}}/K_m$ for aminopyrrolnitrin oxygenation fits Equation 1, which describes a bell-shaped curve with slopes equal to 1, is bell-shaped, and is dependent on two ionizing groups, indicating that a group with a pK of ~ 6.8 on the acidic side of the curve has to be deprotonated and a group with a pK of ~ 8.9 on the basic side of the curve has to be protonated for activity. The fit indicated a correlation coefficient R^2 value of 0.986. In the $\log k_{\text{cat}}$ versus pH plot, $\log k_{\text{cat}}$ increased steadily up to pH 8.0 and then decreased with a slope less than 0.3.

Substrate Specificity—In air-saturated buffer at 30 $^\circ\text{C}$, the concentration of oxygen in solution is 247 μM (43), *i.e.* ~ 10 -fold the K_{O_2} values (27 μM or below) determined with arylamines (TABLE ONE), ensuring that most enzymes are saturated with oxygen. Consequently, both the apparent k_{cat} and k_{cat}/K_m values determined at atmospheric oxygen with arylamines approximate well the values that would be measured by

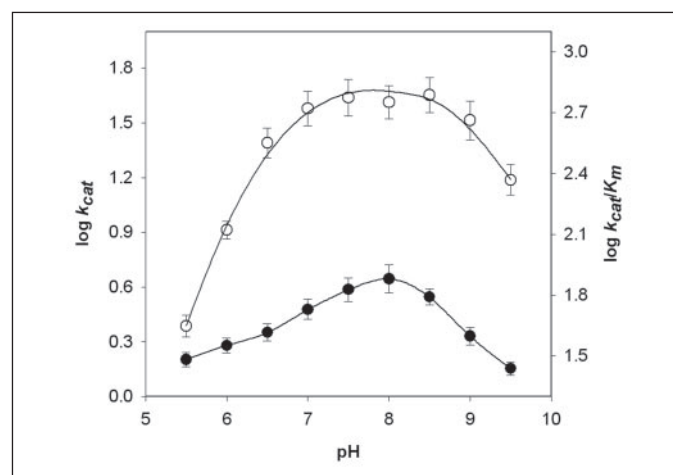


FIGURE 6. pH dependence of steady state kinetic parameters, $\log k_{\text{cat}}$ (●), and $\log k_{\text{cat}}/K_m$ (○) of PrnD with aminopyrrolnitrin as substrate. PrnD activity was measured at 30 $^\circ\text{C}$ in the presence of NADPH, FMN, and SsuE, as described under "Experimental Procedures."

TABLE ONE

Substrate specificity of aminopyrrolnitrin oxygenase (PrnD)

Enzyme activity was measured as described under "Experimental Procedures" at varying concentrations of organic substrates in air-saturated 20 mM Tris-CCl (pH 7.8) at 30 $^\circ\text{C}$. Other substrate analogues mentioned under "Experimental Procedures" did not show any significant conversion into the corresponding nitro products. K_m is the Michaelis constant for the organic substrate. K_m under O_2 is the Michaelis constant for oxygen.

Substrate	k_{cat}	K_m	k_{cat}/K_m	O_2	
				K_m	k_{cat}/K_m
	min^{-1}	μM	$\mu\text{M}^{-1} \text{min}^{-1}$	μM	$\mu\text{M}^{-1} \text{min}^{-1}$
Aminopyrrolnitrin	6.8 ± 0.59	191 ± 20	0.036 ± 0.004	19 ± 2.5	0.121 ± 0.016
<i>p</i> -Aminobenzyl amine	6.5 ± 0.62	379 ± 34	0.017 ± 0.002	27 ± 3.2	0.087 ± 0.011
<i>p</i> -Aminobenzyl alcohol	1.8 ± 0.20	42.2 ± 3.8	0.043 ± 0.005	22 ± 1.9	0.034 ± 0.004
<i>p</i> -Aminophenyl alanine	1.2 ± 0.16	35.5 ± 3.1	0.033 ± 0.004	24 ± 2.2	0.019 ± 0.003

varying the concentration of both organic substrate and oxygen. As expected based on this analysis, the k_{cat} and k_{cat}/K_m determined with the arylamines at atmospheric oxygen were similar to those determined by varying the concentration of oxygen (data not shown). PrnD revealed a high substrate specificity toward physiological substrate aminopyrrolnitrin, *p*-aminobenzyl amine, *p*-aminobenzyl alcohol, and *p*-aminophenyl alanine. 4-Aminobenzamide was slightly converted, and none of 15 other compounds tested was converted. The more extensive kinetic analyses are consistent with a narrow range of substrate specificity, as indicated by k_{cat}/K_m that reflects the relative selectivity of the enzyme for different substrates (TABLE ONE). Interestingly, the specificity of the enzyme for arylamines seems to be independent of the size of the substrate, because the k_{cat}/K_m value for aminopyrrolnitrin was similar to those for *p*-aminobenzyl alcohol and *p*-aminophenyl alanine and 2-fold higher than that for *p*-aminobenzyl amine. Furthermore, substrate size does not significantly affect the overall enzymatic rate of turnover, as shown by the k_{cat} values seen within the similar structure of arylamines and the different structure of arylamines.

Effect of Superoxide Dismutase, Catalase, and Xanthine Oxidase on PrnD Activity—The binding of dioxygen to iron at the active site can produce superoxide by attracting one electron from the active site iron and can produce a peroxide by attracting one electron from the active site iron and one from the Rieske center. Such species could attack substrate bound in the substrate pocket and form a covalent bond to the substrate. Thus, the oxidation of an arylamine to an aryl nitro group can be catalyzed via a nonenzymatic free radical chain reaction that is initiated and propagated by superoxide. If this were the case, one would expect the rate of oxygenation to decrease significantly when the enzymatic activity of PrnD is measured in the presence of superoxide dismutase, because the superoxide would be converted to oxygen and hydrogen peroxide. Consequently, the effect of superoxide dismutase on the reaction catalyzed by PrnD with substrates was determined. With both substrates tested, aminopyrrolnitrin and *p*-aminobenzyl amine, the rate of oxygenation did not change when superoxide dismutase was present in the reaction mixture at a concentration range of 10–100 $\mu\text{g}/\text{ml}$. The catalase and xanthine/xanthine oxidase systems, which generates both superoxide and hydrogen peroxide, were used to further investigate the involvement of superoxide or hydrogen peroxide in the oxygenation. Inhibition of pyrrolnitrin formation by catalase and xanthine oxidase was variable but was always less than 10% up to 100 $\mu\text{g}/\text{ml}$.

Hydroxyl radicals produced either via a Haber-Weiss reaction or a Fenton-type reaction could also participate in the oxidation process. To test this possibility, incubations of aminopyrrolnitrin with the PrnD system were performed in the presence of mannitol and Me_2SO , which have been found to be effective as hydroxyl radical scavengers (44). At the concentrations used in the experiments (0–100 mM), neither mannitol nor Me_2SO affected PrnD activity. Thus, it appears unlikely that the oxidation of aminopyrrolnitrin to pyrrolnitrin is mediated by hydroxyl radicals. Taken together, these results are consistent with the oxidation of the arylamine substrates catalyzed by PrnD occurring at the enzyme active site and not involving a free radical chain reaction.

Investigation of the Origin of Oxygen with $^{18}\text{O}_2$ and H_2^{18}O —To confirm whether indeed molecular oxygen was the substrate of the PrnD reaction and whether one or both oxygen atoms of O_2 were incorporated into the product, isotope labeling experiments with $^{18}\text{O}_2$ were carried out. Incorporation of the label was analyzed by liquid chromatography coupled to electrospray ionization mass spectrometry analysis. Reconstituted PrnD was incubated with aminopyrrolnitrin under an atmosphere of $^{18}\text{O}_2$. A control incubation was carried out under the

usual $^{16}\text{O}_2$ atmosphere. The reaction product pyrrolnitrin was separated by HPLC and analyzed by electrospray ionization mass spectrometry. Fig. 7 shows the molecular ions obtained in a usual $^{16}\text{O}_2$ atmosphere (Fig. 7A) and in $^{18}\text{O}_2$ atmosphere (Fig. 7B). Unlabeled pyrrolnitrin showed the molecular ion at $[\text{M}+\text{H}]^+ = 257$ under the $^{16}\text{O}_2$ atmosphere. In contrast, most of the pyrrolnitrin produced under the $^{18}\text{O}_2$ atmosphere showed the molecular ion at $[\text{M}+\text{H}]^+ = 261$, indicating the incorporation of two ^{18}O atoms. Exchange of $^{18}\text{O}_2$ with water was not observed, although it has been reported to take place with some other non-heme iron-containing oxygenases (45). PrnD was also incubated with aminopyrrolnitrin in labeled water H_2^{18}O . A control incubation was carried out in the usual buffer. In contrast to $^{18}\text{O}_2$ incorporation, pyrrolnitrin produced in H_2^{18}O showed the molecular ion at $[\text{M}+\text{H}]^+ = 257$. Hence, the oxygen atoms in the pyrrolnitrin product are derived exclusively from molecular oxygen O_2 , not from H_2O .

Overall Reaction in PrnD—The consensus Rieske sequence motif CXHX_{15–17}CXXH in PrnD identified by sequence alignment (see supplemental material) of over 80 genes sharing homology to PrnD suggests that the two atoms of iron are coordinated by Cys⁶⁹ and Cys⁸⁸ and His⁷¹ and His⁹¹, respectively (Fig. 8A). Site-directed mutagenesis confirmed the indispensable role of Cys⁶⁹ and Cys⁸⁸ in catalysis because both C69A and C88A PrnD mutants lost their activity (below 0.1%), and the [2Fe-2S] EPR signal is completely absent from the spectra of two cysteine mutants. These results unambiguously confirm the requirement of two cysteine residues for iron sulfur cluster formation in PrnD. The other highly conserved motif in PrnD is DXXHXXXXXH involved in the formation of a mononuclear non-heme Fe(II) catalytic site that is believed to be the site of dioxygen activation and substrate oxygenation in Rieske oxygenases (19, 46). Sequence alignment between PrnD and the Rieske dioxygenase with a crystal structure, naphthalene dioxygenase α -subunit suggests that (i) His¹⁸⁶, His¹⁹¹, and Asp³²³ are involved in the formation of the recurring 2-His-1-carboxylate facial triad structural motif conserved in all known non-heme Fe(II) oxygenases as shown in Fig. 8A (19), and (ii) Asp¹⁸³, the equivalent residue of D205 in naphthalene dioxygenase α -subunit (47), is involved in electron transfer from the Rieske cluster to the non-heme iron center during catalysis. The indispensable role of these two aspartate residues in catalysis was further confirmed by site-directed mutagenesis. Indeed, upon site-directed mutagenesis of Asp³²³ and Asp¹⁸³ into alanine, their activity was significantly decreased for both D323A (~3%) and D183A (below 0.1%) PrnD mutants. The spectra of the reduced two mutants (D323A and D183A) still exhibit the $g_x = 1.78$, $g_y = 1.89$, and $g_z = 2.03$ features, showing that the [2Fe-2S] center is present in two mutants. With D323A the amplitude of the [2Fe-2S] signal is essentially the same as in the wild type enzyme. With D183A the amplitude is slightly smaller, but g value resonances are still clearly discernible. The overall sequential enzyme reaction and electron transfer for PrnD was illustrated in Fig. 8B.

DISCUSSION

The multi-component oxygenases including Rieske oxygenase seem to be widely distributed within the bacterial world and used in a large variety of biosynthetic and metabolic reactions (19). However, whereas the flavin reductase component of these systems has been the subject of detailed mechanistic and structural studies, very little is known on the oxygenase component, where the oxidation takes place. Especially in the case of arylamine oxygenase including PrnD, there is no information regarding enzyme characteristics and structure. The involvement of PrnD in the biosynthesis of pyrrolnitrin was suggested *in vivo* by a gene inactivation experiment (48). However, because of the general difficulties in expressing and purifying PrnD enzyme, coupled with the lack of

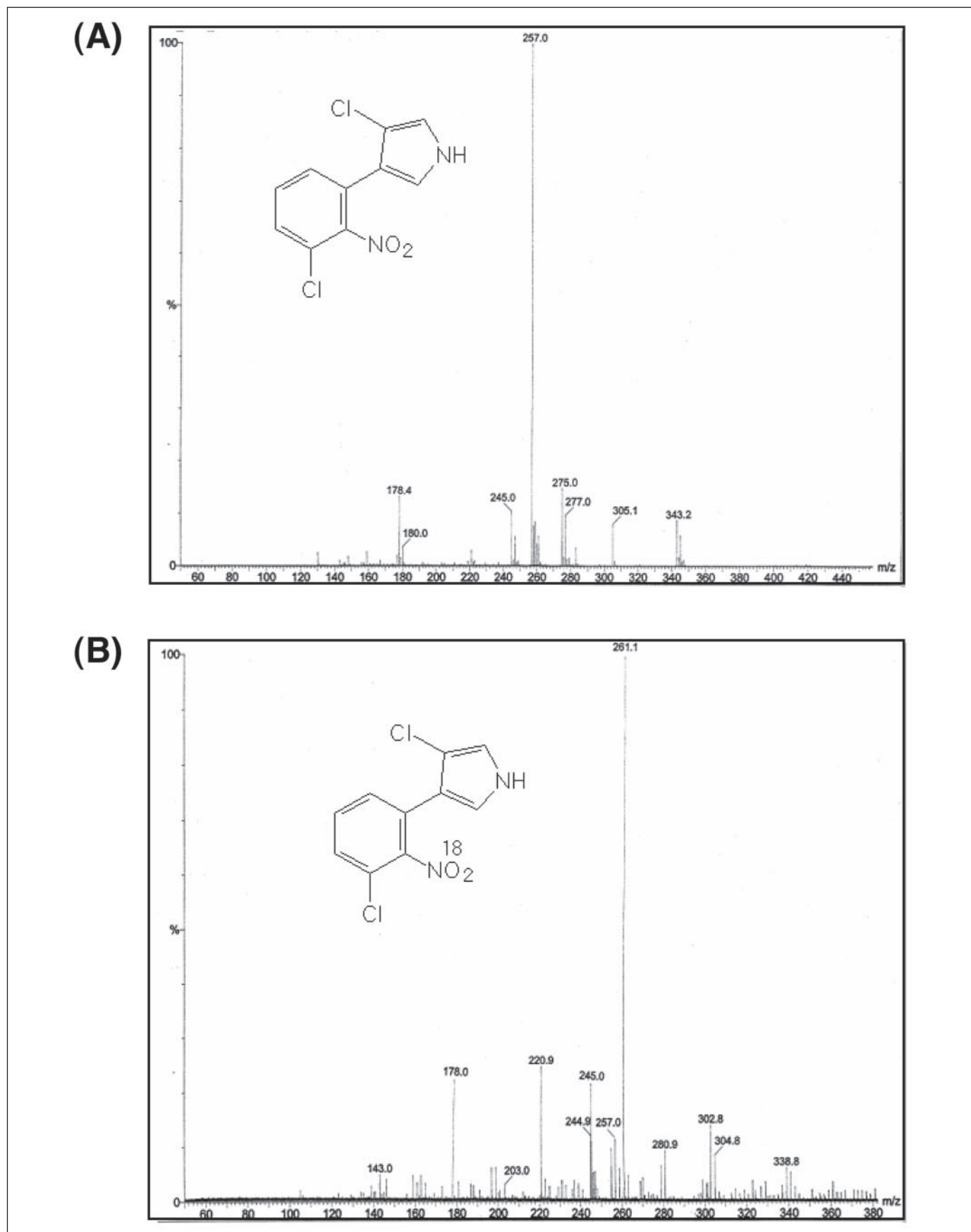


FIGURE 7. Isotope labeling experiments of PrnD with $^{18}\text{O}_2$. A, molecular ion of the reaction product of PrnD with aminopyrrolnitrin under unenriched atmosphere. B, molecular ion under $^{18}\text{O}_2$ -enriched atmosphere. The reaction product of PrnD with aminopyrrolnitrin was separated by HPLC and analyzed by electrospray ionization mass spectrometry.

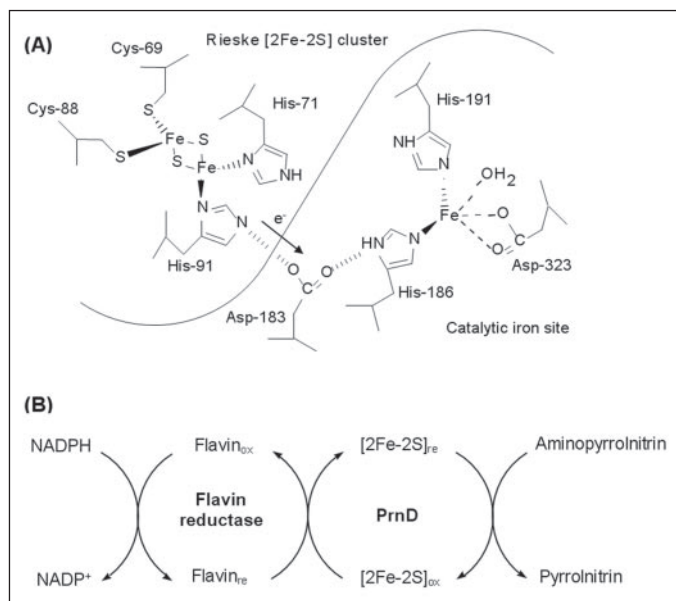


FIGURE 8. A, schematic structure of the Rieske site and non-heme catalytic iron site in PrnD. B, biochemical organization of the PrnD system. A flavoprotein reductase accepts electrons from NADPH and transfers them to PrnD. The reduced PrnD catalyzes the oxygenation of aminopyrrolnitrin to pyrrolnitrin.

commercial substrates required for biochemical studies, so far PrnD has never been characterized and assigned to a defined function by *in vitro* oxygenation. The present results now allow the formulation of a detailed hypothesis for the formation of pyrrolnitrin.

Although PrnD has been suggested to contain [2Fe-2S] clusters, no experimental evidence has been available. In this study, we have succeeded in overexpressing the soluble forms of the PrnD protein in *E. coli* by co-expressing with MBP, which is known to help proteins of interest undergo proper folding *in vivo*. Incubation of the PrnD cleaved from MBP-PrnD fusion protein with reduced iron and sulfide under anaerobic conditions allowed highly efficient reconstitution (2.9 atoms of iron/mol of PrnD subunit, more than 95% of the expected amounts) of the redox-active Rieske-type [2Fe-2S] center *in vitro* as demonstrated by the $g_x = 1.78$, $g_y = 1.89$, and $g_z = 2.03$ EPR spectrum ($g_{av} = (g_x + g_y + g_z)/3 \approx 1.90$) detected at 15 K (Fig. 5). This spectrum is typical of the highly characteristic, rhombic EPR spectra displayed by Rieske [2Fe-2S] clusters (49, 50). Plant-type [2Fe-2S] ferredoxins such as those found in cyanobacteria (25) and the ferredoxin centers of some bacterial dioxygenases (35) also display rhombic EPR spectra, but with g values at about $g_x = 1.89$, $g_y = 1.96$, and $g_z = 2.05$ ($g_{av} \approx 1.96$). In addition, the redox midpoint potential of 95 mV (at pH 7) for the $g_{av} = 1.91$ [2Fe-2S] cluster from PrnD lies well in the range of potentials obtained so far for Rieske proteins (51, 52).

During the reconstitution, proteins were allowed to refold in the presence of reduced iron and sulfide and finally exposed to aerobic buffer in the absence of reducing agents as suggested by Cheng *et al.* (26). Exposure to oxidizing conditions may stabilize the Rieske [2Fe-2S] cluster by allowing formation of the disulfide predicted by the previous studies (53–55). Although other proteins containing the Rieske [2Fe-2S] center such as the Nostoc Rieske protein (56) were reconstituted, this is the first report of reconstitution and characterization of a novel Rieske *N*-oxygenase PrnD catalyzing unusual arylamine oxygenation.

Substrate specificity of PrnD enzyme seems to be independent of the size of substrate, based on the effect of the substrate size on the k_{cat}/K_m and k_{cat} values with several substrates. This independence of the size of substrate were also found in other oxygenases (57–59), suggesting that

the position of the functional group may be more important than the size of the substrate. Thus, with PrnD, it can be proposed that substrate binding occurs at a hydrophobic site large enough to accommodate arylamine substrates with up to at least two aromatic rings, such as aminopyrrolnitrin.

The chloroperoxidase from *P. pyrrocinia* was thought to catalyze the oxidation of arylamine based on the finding that this enzyme catalyzed the *in vitro* oxidation of the amino group of aminopyrrolnitrin to the nitro group of pyrrolnitrin, strongly suggesting the involvement of this enzyme in pyrrolnitrin biosynthesis (60). However, definite proof that no haloperoxidase type of enzyme was involved in the biosynthesis of pyrrolnitrin was obtained by a gene disruption experiment. Even after disruption of the haloperoxidase gene in a *P. fluorescens* strain, this strain still produced pyrrolnitrin (48). Instead, this oxidation is more likely to be catalyzed by a Rieske oxygenase, as suggested by the homology of PrnD with these enzymes (8). Based on the results of the present studies, now it is clear that this oxidation is catalyzed by PrnD, a Rieske *N*-oxygenase as demonstrated by *in vitro* oxygenation of aminopyrrolnitrin into pyrrolnitrin.

In contrast to the halogenation reaction catalyzed by PrnA or PrnC, the catalytic mechanism of PrnD is still unknown. However, by analogy to the mechanisms for *N*-oxidation of arylamines catalyzed by cytochrome P-450 (15), chloroperoxidases (61), and chemical catalysts (62), a putative mechanism for bioconversion of aminopyrrolnitrin to pyrrolnitrin by PrnD may be proposed. The incorporation of the oxygen requires the activation by iron (63, 64). Activated oxygen species or iron peroxo or hydroperoxo intermediates (28, 65) at the non-heme catalytic site can attack nitrogen and following concerted oxygen transfer from the high valent iron-oxo species suggested in cytochrome P-450 (63, 66), phthalate dioxygenase (63), putidamonoxin (63), naphthalene dioxygenase (28), and methane monooxygenase (64, 67) to the nitrogen may produce aromatic nitro-metabolite pyrrolnitrin.

In summary, in the present study the gene coding for PrnD from *P. fluorescens* Pf5 was cloned and heterologously expressed in *E. coli*. The resulting enzyme that catalyzes unusual arylamine oxidation was purified, reconstituted, and found to be a homodimer containing 1 mol of Rieske [2Fe-2S] center and 1 mol of mononuclear iron site/mol of subunit. With arylamines such as aminopyrrolnitrin and *p*-aminobenzyl amine, substrate oxidation occurs at the enzyme active site. A steady state kinetic analysis showed that the preferred substrate for the enzyme is physiological aminopyrrolnitrin and that the enzyme has narrow substrate specificity. From a mechanistic standpoint, PrnD operates through a dioxygenase-like catalytic mechanism, in which molecular dioxygen is incorporated into the substrate based on the results of isotope labeling experiments with $^{18}\text{O}_2$. To our knowledge, this represents the first account in which arylamine compounds are formed from arylamine substrate *in vitro* catalyzed by a Rieske *N*-oxygenase. Additionally, a single gene encoding an arylamine oxygenase has never been expressed in heterologous hosts and has never been characterized. The availability of large amounts of recombinant active PrnD will be instrumental for detailed mechanistic and structural studies aimed at a better understanding of the chemical mechanism of oxidation of arylamine catalyzed by PrnD. Our results should improve understanding of arylamine oxidation in biological processes. In addition, PrnD may be used to synthesize a variety of aromatic nitro compounds from the corresponding aromatic amines, thus adding a new powerful tool into the toolbox of industrial biocatalysis.

Acknowledgment—We thank Dr. John W. Frost for providing aminopyrrolnitrin and helpful discussions.

Characterization of Aminopyrrolnitrin Oxygenase

REFERENCES

1. Arima, K., Imanaka, H., Kousaka, M., Fukuda, A., and Tamura, G. (1965) *J. Antibiot. (Tokyo)* **18**, 201–204
2. Nishida, M., Matsubara, T., and Watanabe, N. (1965) *J. Antibiot. (Tokyo)* **18**, 211–219
3. Burkhead, K. D., Schisler, D. A., and Slininger, P. J. (1994) *Appl. Environ. Microbiol.* **60**, 2031–2039
4. Lambert, B., Leyns, F., Vanrooyen, L., Gossele, F., Papon, Y., and Swings, J. (1987) *Appl. Environ. Microbiol.* **53**, 1866–1871
5. Pfender, W. F., Kraus, J., and Loper, J. E. (1993) *Phytopathology* **83**, 1223–1228
6. Lambowitz, A. M., and Slayman, C. W. (1972) *J. Bacteriol.* **112**, 1020–1022
7. Jespers, A. B. K., and Dewaard, M. A. (1995) *Pesticide Sci.* **44**, 167–175
8. Hammer, P. E., Hill, D. S., Lam, S. T., VanPee, K. H., and Ligon, J. M. (1997) *Appl. Environ. Microbiol.* **63**, 2147–2154
9. Kirner, S., Hammer, P. E., Hill, D. S., Altmann, A., Fischer, I., Weislo, L. J., Lanahan, M., van Pée, K. H., and Ligon, J. M. (1998) *J. Bacteriol.* **180**, 1939–1943
10. van Pée, K. H., Salcher, O., and Lingens, F. (1980) *Angew. Chem. Int. Ed. Engl.* **19**, 828–829
11. Morris, M., Pagan, G., and Warmke, H. (1954) *Science* **119**, 322–323
12. Rebstock, C., Crooks, H. J., Controulis, J., and Bartz, Q. (1949) *J. Am. Chem. Soc.* **71**, 2458–2462
13. Lancini, G. C., Kluepfel, D., Lazzari, E., and Sartori, G. (1966) *Biochim. Biophys. Acta* **130**, 37–44
14. King, R. R., Lawrence, C. H., and Calhoun, L. A. (1998) *Phytochemistry* **49**, 1265–1267
15. Meunier, B., de Visser, S. P., and Shaik, S. (2004) *Chem. Rev.* **104**, 3947–3980
16. He, J., and Hertweck, C. (2004) *J. Am. Chem. Soc.* **126**, 3694–3695
17. Winkler, R., and Hertweck, C. (2005) *Angew. Chem. Int. Ed. Engl.* **44**, 4083–4087
18. van Pée, K. H., and Ligon, J. M. (2000) *Nat. Prod. Rep.* **17**, 157–164
19. Costas, M., Mehn, M. P., Jensen, M. P., and Que, L. (2004) *Chem. Rev.* **104**, 939–986
20. Resnick, S. M., Lee, K., and Gibson, D. T. (1996) *J. Ind. Microbiol. Biotechnol.* **17**, 438–457
21. Sambrook, J., Fritsch, E. F., and Maniatis, T. (1989) *Molecular Cloning: A Laboratory Manual*, 2nd Ed., Cold Spring Harbor Laboratory, Cold Spring Harbor, NY
22. Kim, Y. W., Choi, J. H., Kim, J. W., Park, C., Kim, J. W., Cha, H. J., Lee, S. B., Oh, B. H., Moon, T. W., and Park, K. H. (2003) *Appl. Environ. Microbiol.* **69**, 4866–4874
23. Kim, I. C., Cha, J. H., Kim, J. R., Jang, S. Y., Seo, B. C., Cheong, T. K., Lee, D. S., Choi, Y. D., and Park, K. H. (1992) *J. Biol. Chem.* **267**, 22108–22114
24. Yano, T., Sled, V. D., Ohnishi, T., and Yagi, T. (1996) *J. Biol. Chem.* **271**, 5907–5913
25. Cheng, H., Xia, B., Reed, G. H., and Markley, J. L. (1994) *Biochemistry* **33**, 3155–3164
26. Cheng, H., Westler, W. M., Xia, B., Oh, B. H., and Markley, J. L. (1995) *Arch. Biochem. Biophys.* **316**, 619–634
27. Yano, T., Magnitsky, S., Sled, V. D., Ohnishi, T., and Yagi, T. (1999) *J. Biol. Chem.* **274**, 28598–28605
28. Wolfe, M. D., Parales, J. V., Gibson, D. T., and Lipscomb, J. D. (2001) *J. Biol. Chem.* **276**, 1945–1953
29. Gong, X. M., and Carmeli, C. (2003) *Anal. Biochem.* **321**, 259–262
30. Mason, J. R., and Cammack, R. (1992) *Annu. Rev. Microbiol.* **46**, 277–305
31. Keller, S., Wage, T., Hohaus, K., Holzer, M., Eichhorn, E., and van Pée, K. H. (2000) *Angew. Chem. Int. Ed. Engl.* **39**, 2300–2302
32. Fee, J. A., Findling, K. L., Yoshida, T., Hille, R., Tarr, G. E., Hearshen, D. O., Dunham, W. R., Day, E. P., Kent, T. A., and Munck, E. (1984) *J. Biol. Chem.* **259**, 124–133
33. Malkin, R. (1973) in *Iron-Sulfur Proteins* (Lovenberg, W., ed) pp. 1–26, Academic Press, New York
34. Fee, J. A., Kuila, D., Mather, M. W., and Yoshida, T. (1986) *Biochim. Biophys. Acta* **853**, 153–185
35. Riedel, A., Fetzner, S., Rampp, M., Lingens, F., Liebl, U., Zimmermann, J. L., and Nitschke, W. (1995) *J. Biol. Chem.* **270**, 30869–30873
36. Kerschler, L., Oesterheld, D., Cammack, R., and Hall, D. O. (1976) *Eur. J. Biochem.* **71**, 101–107
37. Lubben, M., Arnaud, S., Castresana, J., Warne, A., Albracht, S. P. J., and Saraste, M. (1994) *Eur. J. Biochem.* **224**, 151–159
38. Yamaguchi, M., and Fujisawa, H. (1982) *J. Biol. Chem.* **257**, 12497–12502
39. Yamaguchi, M., and Fujisawa, H. (1980) *J. Biol. Chem.* **255**, 5058–5063
40. Geary, P. J., Mason, J. R., and Joannou, C. L. (1990) *Methods Enzymol.* **188**, 52–60
41. Crutcher, S. E., and Geary, P. J. (1979) *Biochem. J.* **177**, 393–400
42. Batie, C. J., LaHaie, E., and Ballou, D. P. (1987) *J. Biol. Chem.* **262**, 1510–1518
43. Salcher, O., Lingens, F., and Fischer, P. (1978) *Tetrahedron Lett.* **34**, 3097–3100
44. Cederbaum, A. I., Dicker, E., and Cohen, G. (1978) *Biochemistry* **17**, 3058–3064
45. Baldwin, J. E., Adlington, R. M., Crouch, N. P., and Pereira, I. A. C. (1993) *Tetrahedron* **49**, 7499–7518
46. Bertini, I., Cremonini, M. A., Ferretti, S., Lozzi, I., Luchinat, C., and Viezzoli, M. S. (1996) *Coordination Chem. Rev.* **151**, 145–160
47. Kauppi, B., Lee, K., Carredano, E., Parales, R. E., Gibson, D. T., Eklund, H., and Ramaswamy, S. (1998) *Structure* **6**, 571–586
48. Kirner, S., Krauss, S., Sury, G., Lam, S. T., Ligon, J. M., and vanPee, K. H. (1996) *Microbiology (Read.)* **142**, 2129–2135
49. Rieseke, J. S., Hansen, R. E., and Zaugg, W. S. (1964) *J. Biol. Chem.* **239**, 3017–3022
50. Malkin, R., and Aparicio, P. J. (1975) *Biochem. Biophys. Res. Commun.* **63**, 1157–1160
51. Cammack, R. (1984) in *Charge and Field Effects in Biosystems* (Allen, M. J., and Usherwood, P. N. R., eds) pp. 41–51, Abacus Press, Tunbridge Wells, UK
52. Kuila, D., and Fee, J. A. (1986) *J. Biol. Chem.* **261**, 2768–2771
53. Graham, L. A., and Trumpower, B. L. (1991) *J. Biol. Chem.* **266**, 22485–22492
54. Davidson, E., Ohnishi, T., Attaafoadjei, E., and Daldal, F. (1992) *Biochemistry* **31**, 3342–3351
55. Iwata, S., Saynovits, M., Link, T. A., and Michel, H. (1996) *Structure* **4**, 567–579
56. Holton, B., Wu, X., Tsapin, A. I., Kramer, D. M., Malkin, R., and Kallas, T. (1996) *Biochemistry* **35**, 15485–15493
57. Lessner, D. J., Johnson, G. R., Parales, R. E., Spain, J. C., and Gibson, D. T. (2002) *Appl. Environ. Microbiol.* **68**, 634–641
58. Parales, J. V., Parales, R. E., Resnick, S. M., and Gibson, D. T. (1998) *J. Bacteriol.* **180**, 1194–1199
59. McKay, D. B., Prucha, M., Reineke, W., Timmis, K. N., and Pieper, D. H. (2003) *J. Bacteriol.* **185**, 2944–2951
60. Kirner, S., and Vanpee, K. H. (1994) *Angew. Chem. Int. Ed. Engl.* **33**, 352–352
61. Doerge, D. R., and Corbett, M. D. (1991) *Chem. Res. Toxicol.* **4**, 556–560
62. Murray, R. W., Jeyaraman, R., and Mohan, L. (1986) *Tetrahedron Lett.* **27**, 2335–2336
63. Que, L., Jr., and Ho, R. Y. (1996) *Chem. Rev.* **96**, 2607–2624
64. Wallar, B. J., and Lipscomb, J. D. (1996) *Chem. Rev.* **96**, 2625–2658
65. Bassan, A., Blomberg, M. R., and Siegbahn, P. E. (2004) *J. Biol. Inorg. Chem.* **9**, 439–452
66. Ortiz de Montellano, P. R. (2005) *Cytochrome P-450: Structure, Mechanism, and Biochemistry*, 3rd Ed., Kluwer Academic/Plenum Publishers, New York
67. Fox, B. G., Borneman, J. G., Wackett, L. P., and Lipscomb, J. D. (1990) *Biochemistry* **29**, 6419–6427